(Received 1 April 2024, Accepted 27 May 2024, Scheduled 8 June 2024)

Design of Superconducting H-Shaped Microstrip Antennas on Anisotropic Substances Using Hybrid Cavity Model

Mohamed Bedra[1], Djemai Arar[1], Djamel Benatia[1], Sami Bedra[1, 2, *], and Akram Bediaf[1]

[1] *Laboratory of Advanced Eectronics (LEA), Department of Electronics, University of Batna2, Batna 05000, Algeria*
[2] *Department of Industrial Engineering, University of Khenchela, Khenchela 40004, Algeria*

ABSTRACT: This study investigates the effects of various antenna parameters, such as the substrate material, thickness of the superconducting patch, and operating temperature, on the resonance frequency and surface resistance/reactance of an H-shaped patch antenna printed on a uniaxial anisotropic substrate using a hybrid cavity model and fabricated with superconductor material. This model stands out for its simplified mathematical approach and cost effectiveness. Importantly, the numerical results demonstrate a high level of agreement with the experimental findings reported in the literature, reinforcing the reliability of our study. Additionally, other numerical results demonstrate the impact of the superconductivity materials on the resonant characteristics of the H-shaped compact microstrip antenna.

1. INTRODUCTION

Recently, there has been significant interest in the development and use of high-temperature superconducting materials. Various researches have highlighted the substantial energy waste in the millimeter range, particularly when the patch material is a normal conductor. To reduce energy waste and enhance efficiency, we need to employ patches based on superconducting materials [1]. Microstrip antennas (MSAs) are highly used in aerospace applications due to their low weight, compact size, and compatible nature. Rectangular and circular disc antennas are the most common types of microstrip antennas [2]. Depending on the application, we also put into consideration other small chip antennas. We present two alternatives to the rectangular patch antenna. In addition to that extensive applications in various microwave systems, such as wireless equipment, missiles, satellites, and sensors are being developed [3]. The resonance frequency of the small ribbon antenna relied on the geometry, dimensions, and electrical insulation constant of the substrate. Determining the resonance frequency of the antenna focuses on its physical parameters, forming the basis for the analysis process. Transmission line, cavity method (analytical), and full-wave method (numerical) are the predominant methods of analysis [2, 3]. The first mentioned method is the most accurate. Acknowledging the resonance frequency helps in determining certain physical parameters of the antenna during the design analysis process. Accuracy in determining these parameters are crucial since this type of antenna has a narrow bandwidth. Microstrip antennas or patch antennas are becoming increasingly useful due to their ability to be printed directly on printed circuit board (PCB). The use of microstrip antennas is becoming more common in the mobile phone market. Patch antennas are easy to manufacture thanks to their low profile and cost [4]. The size of the patch antenna, denoted as 'H' in the illustration on (Fig. 1). The experimental findings unambiguously indicate that the H-shaped microstrip patch is notably smaller than conventional half-wavelength rectangular patch antennas and ring antennas [5], has fewer number modes and absence of harmonic resonance [6]. The H-shape antenna contains a ground plane as a basal layer, and above it, we have a substrate which is marked by a dielectric permittivity ε_r and a thickness h. Over the substrate there is a patch with a dimension parameters including: length L, width W, and internal dimension defined by gap length s and gap width d. This structure is approximately half the size of the rectangular patch, featuring a high beamwidth but a narrower bandwidth. In contrast, the rectangular annular antenna has a smaller size, high beamwidth, and a smaller bandwidth. A compact H-shaped patch antenna, owing to its significantly smaller size, can substitute for the rectangular patch at Ultra High Frequency (UHF). When applying it in the frequency range below 2 Gigahertz, small rectangular patch sizes appear comparatively large [7]. Even though many of the substrate materials are regarded as isotropic, but actually they are anisotropic [8]. This anisotropy can be found in composite laminate materials, formerly known as Epsilam-10 [9], and natural materials like sapphire and alumina [10]. The performance of antennas and other devices may be impacted by this anisotropy, regardless of whether it was a planned by product of the manufacturing process [11]. Anisotropic materials are frequently used to enhance the performance of conventional microstrip antennas [12–14]. In our previous research, we showed that selecting the appropriate structural parameters and combining them with the optical properties of anisotropic materials can control the resonant frequency and achieve wider bandwidth characteristics [14]. However, using anisotropic substrate materials on compact antennas has received little attention in the literature. In this work, we first study a superconducting H-shape microstrip antenna. Thus, we use a hybrid approach

* Corresponding author: Sami Bedra (bedra_sami@univ-khenchela.dz).

based on cavity model which is employed for analyzing our structure shown in (Fig. 1). Before understanding the effect of physical parameters on the resonance frequency, we must initially validate our mathematical formulation starting from the equation of the resonance frequency of H-shape microstrip antenna ending in finding the resonance frequency of superconducting patch, in light of our previous discussion; we will verify our findings by comparing them with those of other researchers. Then, we execute a parametric study of the superconducting H-shape MSA, so we create graphical representations based on the characteristics of the superconducting microstrip antenna to illustrate the results obtained through the cavity method. Among these graphics, we investigate the impact of the temperature T and patch thickness t on the resonance frequency. With all of the aforementioned parameters, we utilize two different uniaxial anisotropic materials (Epsilam and Sapphir). Also two types of substrates (Anisotropic and isotropic ones) are used (anisotropic and isotropic). Finally, we are going to study the impact of physical factors, including tolerance and electrical insulation thickness, as well as the aperture width of the radiating element on the resonance properties

2. MATHEMATICAL FORMULATION

To analyze our microstrip patch antenna, we will employ a cavity model. This model facilitates a swift determination of results, starting with the encapsulation of our antennas within the cavity. This cavity model analyzes patches using two electric and four magnetic walls, and a strategic approach is essential. The absence of tangential electric fields $(E_x = 0, E_y = 0)$ is maintained by a ground plane and a perfect electric conductor (PEC) patch. The internal electronic field aligns along the Z-axis $(E = E_z(x, y)k)$. Using the Maxwell's equations and propagation equation leads to a solution for $E_z(x, y)$. The final expression for $E_z(x, y)$ involves constants and cosines, defining the mode characteristics. This model got diversity of dielectric permittivity ε_r and thicknesses h.

The cavity model included a variety of substrate dielectric constants ε_r and thicknesses h. To account for the influence of fringing fields, either effective side length or effective dielectric constant, or both, have been employed to explain recorded resonance frequency and other characteristics. For the same reason, dynamic permittivity has been investigated. When using an effective dielectric constant ε_{eff}, the user must first determine ε_{eff} before estimating the physical side length [15].

2.1. Resonant Frequency

Figure 1 illustrates the geometric and physical dimensions of the H-shaped patch antenna, influencing the resonance frequency of the microstrip antenna. Generally, it is a function of the patch dimensions, the electrical insulation constant of the substrate, and its thickness. The primary rectangular patch resonance frequency mode TM_{10} is crucial in radiation, calculated using the resonator length L and the equations of effective electrical insulation constant ε_{reff}. The extension of the literature is

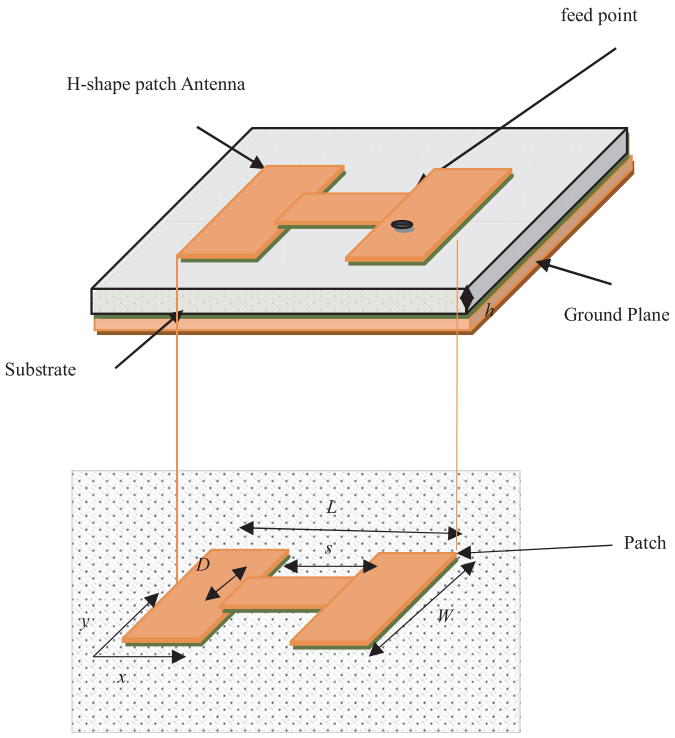

FIGURE 1. Geometry of a H-shaped microstrip antenna.

presented as follows:

$$f_r = \frac{C}{2L_{eff}\sqrt{\varepsilon_{reff}}} \tag{1}$$

with:

$$L_{eff} = L + 2\Delta L \tag{2}$$

Also, with:

$$\Delta L = 0.412h\frac{\varepsilon_r + 0.3}{\varepsilon_r - 0.258}\left(\frac{W/h + 0.264}{W/h + 0.813}\right) \tag{3}$$

C in Equation (1) represents the speed of electromagnetic waves in free space, and irregular medium effects of the rectangular patch are considered in terms of an effective relative insulation constant ε_{reff} along with the boundary effects of electrical fields at the radiating edges of the space. The rectangular area is taken into account by the linear edge extension dimension ΔL. The following equations are provided to approximate Schneider's proposed effective electrical insulation constant [16] and Hammerstad's proposed edge extension [17], which may be incorporated into the above equations:

$$\varepsilon_{reff} = \frac{\varepsilon_r + 1}{2} + \frac{\varepsilon_r - 1}{2}\left[1 + 10\frac{h}{w}\right]^{-1/2} \tag{4}$$

Due to the alteration in resonance length resulting from the transition from a traditional rectangular patch antenna to a compact H-shaped patch antenna, the resonance frequency must be adjusted to account for the change in geometrical characteristics.

TABLE 1. Comparison of the measured, simulated, and calculated resonant frequencies.

No. Antennas	Antenna Parameters						Resonance Frequency (GHz)			
	L (mm)	W (mm)	D (mm)	s (mm)	h (mm)	ε_r	Simulate & Measured [20, 21]	Calculated [22]	Our Result	Error (%)
1	24	38	11	8	1.59	2.2	2.190	2.199	2.202	0.548
2	32.69	33	15	4.09	1.59	2.5	2.170	2.270	2.234	2.949
3	35.54	33	15	26	1.59	2.5	1.970	2.022	1.978	0.406
4	43.59	33	15	15	1.59	2.5	1.590	1.613	1.593	0.189
5	45.08	33	15	26	1.59	2.5	1.550	1.574	1.558	0.516
6	54.6	28	15	26	1.59	2.5	1.390	1.390	1.387	0.216
7	64.16	33	15	26	1.59	2.5	1.130	1.109	1.127	0.265

Consequently, the resonance length L of the antenna in Equation (1) needs to be replaced by L_H, representing the length of the compact H-shaped patch. The equations below are employed to calculate the resonance frequency of a compact antenna in the H-shape configuration:

$$f_r = \frac{C}{2L_{eff}\sqrt{\varepsilon_{reff}}} \tag{5}$$

with:

$$L_{Heff} = L_H + 2\Delta L \tag{6}$$

where L_{Heff} denotes the effective resonance length of the compact-shaped antenna.

To simplify, ε_{reff} and ΔL, as denoted by Equations (3) and (4), respectively, are employed similarly to the small rectangular bar antenna. The primary goal of this work is to establish an expression for the resonance length L_H of the compact H-shape antenna to predict the resonance frequency. The length of the compact H-shape antenna is contingent on the dimensions of the patch (L, W, s, d) and is formulated as follows:

$$L_{Heff} = (0.912L - 0.643s) \cdot \left(\frac{s}{d}\right)^{0.437} + W\left(\frac{L}{d}\right)^{0.726} + \left(\frac{h}{\varepsilon_r}\right) - 0.445L\left(\frac{W}{d}\right) \tag{7}$$

As anisotropy has a significant influence on antenna performance, it is important to consider this effect. The tensor of relative permittivity of uniaxial anisotropic dielectric is given by:

$$\overline{\varepsilon_r} = \begin{bmatrix} \varepsilon_x & 0 & 0 \\ 0 & \varepsilon_y & 0 \\ 0 & 0 & \varepsilon_z \end{bmatrix} \tag{8}$$

with $\varepsilon_x = \varepsilon_y$.

Utilizing electromagnetic knowledge, the thickness h and relative permittivity ε_x and ε_z of the uniaxial anisotropic substrate are replaced by effective parameters using the following equations [18]:

$$\varepsilon_{re} = \varepsilon_z \tag{9}$$

$$h_e = h\sqrt{\frac{\varepsilon_x}{\varepsilon_z}} \tag{10}$$

2.2. Resonance Frequency of a Superconducting Patch

The sudden alteration in the operating frequency (resonance frequency) of the superconducting antenna at a temperature close to T can be associated with a variation by adjusting the London penetration depth (λ_0) (these last λ at null temperature $T = 0\,\mathrm{K}$ of the superconducting material YBCO ($YBa_2Cu_3O_7$). To model the resonance frequency of the superconducting antenna, it is necessary to consider the effective dielectric constant ε_{reff} given by [19]:

$$\varepsilon_{r,eff} = \varepsilon_{re}\left[1 + \frac{\lambda_f}{h}\coth\left(\frac{t}{\lambda_f}\right)\right] \tag{11}$$

t and λ_f signify the superconducting patch thickness and magnetic wavelength, respectively, determined by the Gorter-Casimir two-fluid model [19] and are considered in the analysis.

$$\lambda_f = \lambda_0\left[1 - \left(\frac{T}{T_c}\right)^4\right]^{-1/2} \tag{12}$$

with T and T_c being the temperature and critical temperature of the superconductor, respectively.

3. VALIDATION OF NUMERICAL RESULTS

To validate the accuracy of our calculations, we compared our results with previously published findings [20–22]. The resonance frequencies, calculated using the cavity method described in the preceding section for a H-shape patch antenna printed on an isotropic substrate, are listed alongside the theoretical results available in the literature. In Table 1, our calculated resonance frequency results are compared with the references [20–22]. The comparison shows good alignment between resonance frequencies calculated by our method and those measured, simulated, and calculated for a perfectly conductive H-shaped patch. An accuracy analysis is presented in Table 1.

4. DISCUSSIONS OF NUMERICAL RESULTS

Figure 2 illustrates how a superconducting H-shaped patch antenna's resonance frequency varies based on the temperature at

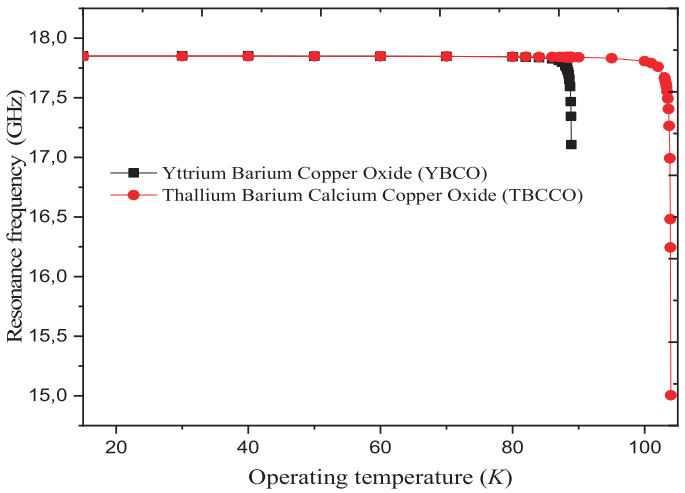

FIGURE 2. Exploring variations in the resonance frequency of an H-shaped superconducting antenna while considering alterations to the operating temperature with two diverse supraconducting materials $\varepsilon_r = 23.6$, $h = 50\,\mu\text{m}$, $L = 985\,\text{nm}$, $W = 1625\,\text{nm}$, $s = 700\,\text{nm}$, $d = 700\,\text{nm}$, $t = 200\,\text{nm}$, $\lambda_0 = 160\,\text{nm}$.

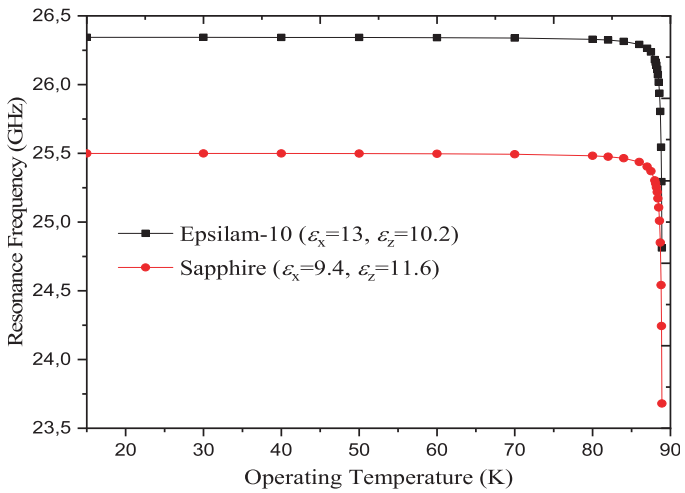

FIGURE 3. Exploring variations in the resonance frequency of an H-shaped superconducting antenna while considering alterations to the operating temperature using two different substrate material $h = 250\,\mu\text{m}$, $L = 985\,\text{nm}$, $W = 1625\,\text{nm}$, $s = 700\,\text{nm}$, $d = 700\,\text{nm}$, $t = 200\,\text{nm}$, $\lambda_0 = 160\,\text{nm}$, $Tc = 89\,\text{K}$.

which it operates. It shows how the resonance frequency of a compact superconducting H-shaped antenna changes with operating temperature when the following parameters are used: relative permittivity $\varepsilon_r = 23.6$ and thickness $h = 50\,\mu\text{m}$. The patch has a size with a length $L = 985\,\text{nm}$ and width $W = 1625\,\text{nm}$, $s = 700\,\text{nm}$, $d = 700\,\text{nm}$, $t = 200\,\text{nm}$, and $\lambda_0 = 160\,\text{nm}$.

It can be noticed that the variations in resonance frequency are relatively reduced with the increase in operating temperature. For YBCO ($YBa_2Cu_3O_7$) material, this reduction becomes more significant for temperature values close to the critical temperature $Tc = 89\,\text{K}$. For the TBBCO ($Tl_2Ba_2CaCu_2O_8$) material, the analysis is carried out in the temperature range of 20 K to 106 K, where Tc is the critical temperature $Tc = 105\,\text{K}$. The resonance frequency decreases slowly for values exceeding $Tc = 105\,\text{K}$. Moreover, these behaviors are very consistent with those reported for the case of a rectangular antenna [23]. Note that the sharp decline in resonance frequency at temperature close to the transition temperature can be attributed to a decrease in magnetic penetration depth [23].

Figure 3 shows a diversity of the resonance frequency of a superconducting H-shape patch antenna printed on a uniaxial anisotropic substrate with the variation of the operating temperature using different substrate materials.

We notice that the variation happened in the resonance frequency is attributed to two factors: elevated in temperature with the gradual decrease of the uniaxial anisotropic substrate. This reduction becomes more significant for temperature values close to the transition temperature (critical temperature) $Tc = 89\,\text{K}$. Additionally, we notice a shift in resonance frequency based on two different substrate materials. One of them is Epsilam-10 with $\varepsilon_x = 13$ and $\varepsilon_z = 10.2$, while the other is Sapphire with $\varepsilon_x = 9.4$ and $\varepsilon_z = 11.6$.

In this figure, it is evident that a higher permittivity or height ratio results in a higher resonance frequency. It is noteworthy that the abrupt change in resonance frequency at temperatures approaching the transition temperature can be associated with an alteration in magnetic field penetration [23].

In Fig. 4, we depict the variation in the resonance frequency of a superconducting compact H-shaped antenna printed on two anisotropic substrates, plotted against the thickness of the superconducting patch. As illustrated in Fig. 4, we investigate the impact of the thickness of the critical high-temperature superconducting film on the resonance frequency. The antenna parameters remain identical to those in the previous preview figure, and the operating temperature is set at $Tc = 75\,\text{K}$. As the patch thickness t increases, the resonance frequency experiences a rapid rise until it reaches λ_0, denoting the penetration depth. Beyond this value, the frequency variation becomes less significant.

The variation in the resonance frequency of an H-shaped superconducting patch antenna, printed on both isotropic and anisotropic substrates is presented in Fig. 5. The thickness of the superconducting patch is an influencing factor. The antenna parameters remain consistent with those employed in Fig. 4. For the isotropic substrate, we use ($\varepsilon_x = \varepsilon_z = 4.83$), and for the anisotropic substrate we use ($\varepsilon_x = 5.5$, $\varepsilon_z = 4.83$), while maintaining an operating temperature of $T = 75\,\text{K}$. It is observed that the resonance frequency increases with the augmentation of the superconducting patch thickness (t). Notably, anisotropy demonstrates more effect on the resonance frequency. Lastly, it is crucial to highlight that the impact of anisotropy is adapted with the increase in the thickness of the superconducting patch (t).

Figure 6(a) displays the surface resistance R_s of an H-shaped antenna with the following parameters: $L = 1320\,\text{nm}$, $W = 1625\,\text{nm}$, $d = 700\,\text{nm}$, $s = 700\,\text{nm}$, $t = 200\,\text{nm}$, and thickness $h = 200\,\mu\text{m}$. The surface resistance R_s is initially observed on an anisotropic substrate ($\varepsilon_x = 9.4$, $\varepsilon_z = 11.6$). The surface resistance values remain constant ideally with value 0 which

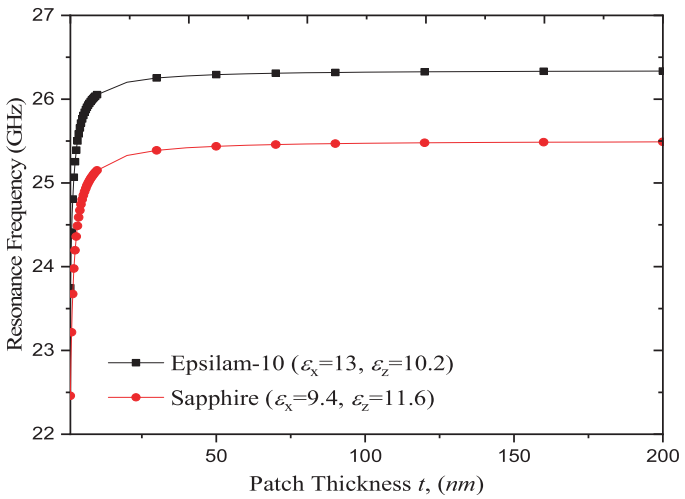

FIGURE 4. Variation of the resonance frequency of a H-shape superconducting antenna printed on anisotropic substrates as per to the thickness of the superconducting patch, with the same parameters as in Fig. 3, at $Tc = 75$ K.

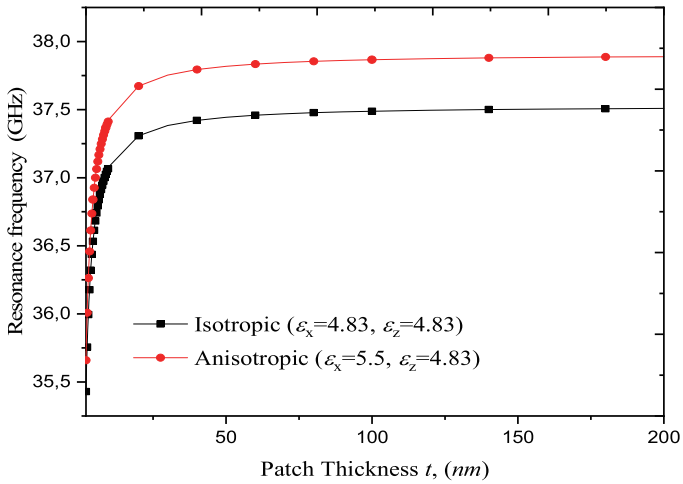

FIGURE 5. Exploring variations in the resonance frequency of an H-shaped superconducting antenna printed on anisotropic/isotropic substrates according to the thickness of the superconducting patch, with the same parameters as in Fig. 4, at $T = 75$ K.

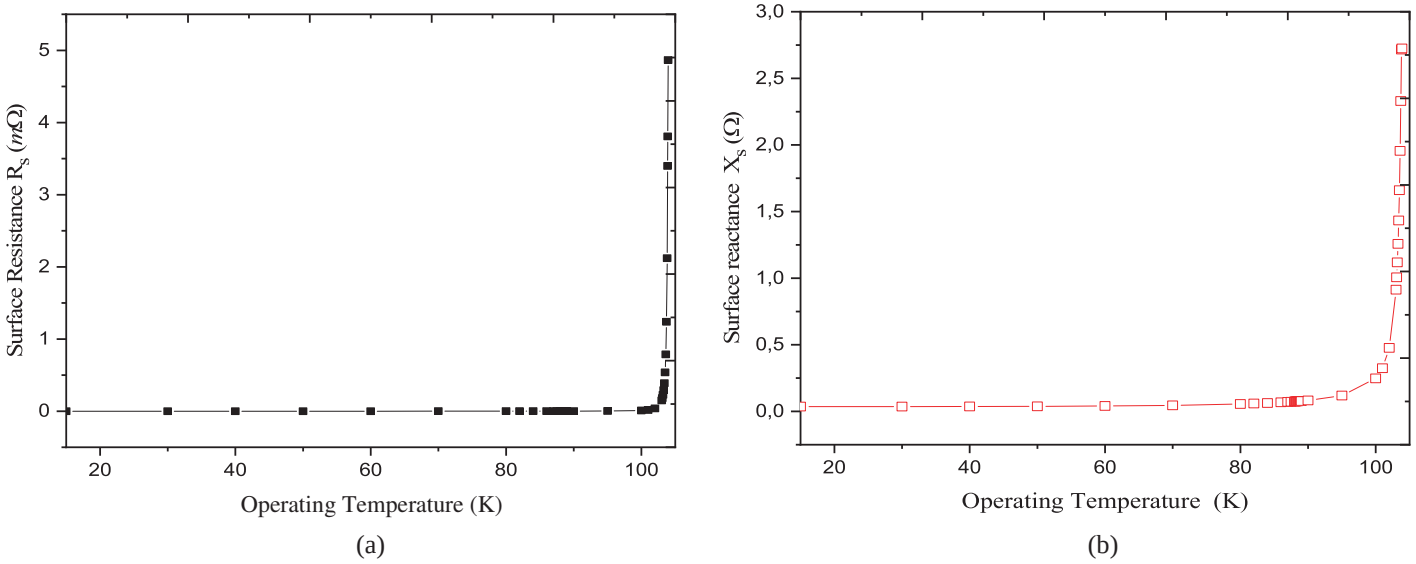

FIGURE 6. Temperature dependence of the surface impedance of an H-shaped superconducting antenna; $h = 200$ µm, $L = 1320$ nm, $W = 1625$ nm, $d = 700$ nm, $s = 700$ nm, $t = 200$ nm, $\lambda_0 = 180$ nm, $Tc = 104$ K, $(\varepsilon_x = 9.4,\ \varepsilon_z = 11.6)$.

means that there is no loss in energy, and the electrical current flows throw the superconductor without resistance at 10 K until reaching the critical temperature $Tc = 104$ K. Beyond a certain point they exhibit a rapid increase in resistance, resulting in both energy loss and a decrease in efficiency.

Figure 6(b) presents the surface reactance X_s with the same parameters as Fig. 6(a). It is observed that within the temperature range of 10 K to 90 K a stable value of 0 is noted indicating a rise in effective magnetic shielding. This suggests a reduction in energy loss, while the reactance increases gradually. The reactance reaches its peak at the critical temperature $Tc = 104$ K, signifying a decrease in effective magnetic shielding. This outcome ultimately contributes to the efficiency of the antenna.

In Fig. 7, we present the surface resistance (a) and surface reactance (b) with the varying in thicknesses t of an H-shaped superconducting antenna. The H-shape has a length $L = 1320$ nm and width $W = 1625$ nm, based on a superconducting material characterized by $\lambda_0 = 180$ nm and $T = 90$ K, printed on a dielectric substrate of thickness $h = 200$ µm and permittivity $(\varepsilon_x = 9.4,\ \varepsilon_z = 11.6)$.

Regarding the results, the surface resistance R_s according to the thickness t of the patch is illustrated in Fig. 7(a). It is observed that when the thickness t of the patch increases, the surface resistance R_s decreases rapidly until the thickness t reaches the penetration depth value λ_0, and the curve remains stable near the value zero.

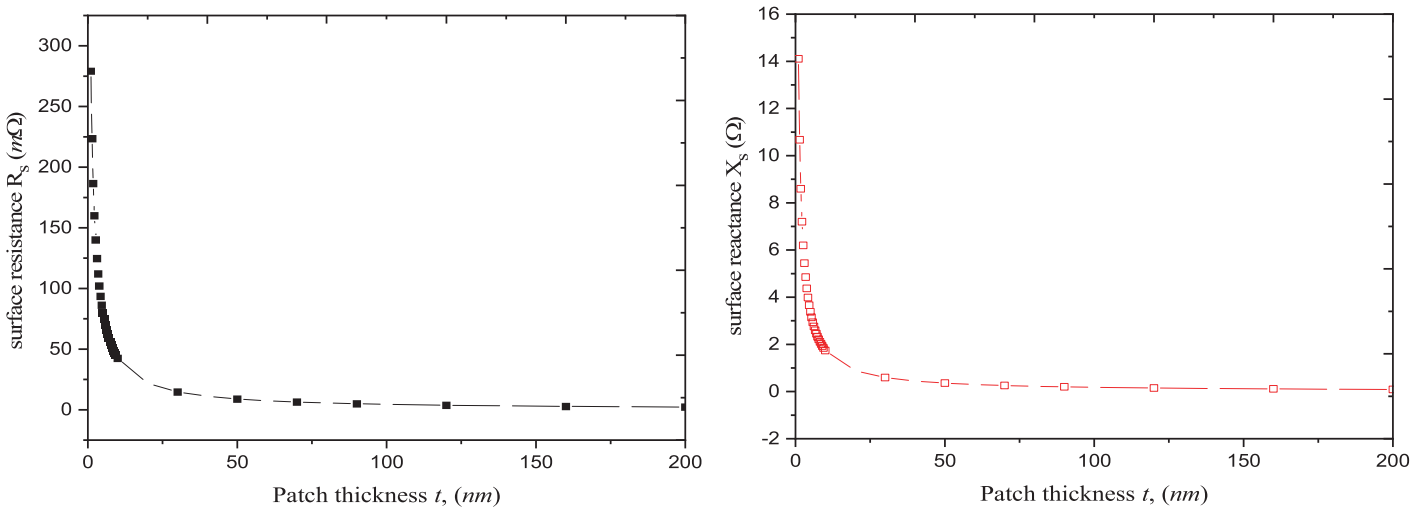

FIGURE 7. Temperature dependence of (a) surface resistance and (b) surface reactance of an H-shaped superconducting antenna. $h = 200\,\mu$m, $L = 1320$ nm, $W = 1625$ nm, $d = 700$ nm, $s = 700$ nm, $T = 90$ K, $\lambda_0 = 180$ nm, $Tc = 104$ K, ($\varepsilon_x = 9.4$, $\varepsilon_z = 11.6$).

Then, the results concerning the surface reactance X_s according to the thickness t of the patch are illustrated in Fig. 7(b). It is also noted that the surface reactance value X_s decreases slowly and in proportion to the increase in the values of the thickness t.

5. CONCLUSION

In this paper, we focus on the effect of the superconductivity on microstrip antennas, leading to significant findings. In this research, a general procedure is employed for the modeling and designing of a compact H-shaped microstrip antenna printed on an anisotropic substrate using the modified cavity method. We examined this structure on a different antenna parameter using various substrate materials, operating temperatures, and patch thicknesses and noticed the alteration in resonance frequency on both surface resistance (R_s)/reactance (X_s). At the beginning, the theoretical findings indicate that the resonance frequency decreases monotonically with the increase of substrate thickness, also a greater decrease observed for a substrate which has higher permittivity. Furthermore, it is demonstrated that the bandwidth increases with the thickness of the substrate, with a more significant increase for a substrate with higher permittivity. Firstly, varying the thickness of the superconducting patch demonstrated a substantial impact on the antenna's resonance frequency. As the patch thickness increased, the resonance frequency exhibited a rapid rise until reaching a critical point; afterward the frequency variation became less evident. This suggests a critical thickness value where the penetration depth influences the antenna's behavior. Moreover, it is noteworthy that the considerable change in resonance frequency at temperatures close to critical one (T_c) can be attributed to the alteration in the magnetic penetration depth of YBCO and TBBCO. Additionally, it is highlighted that selecting the substrate material is important for shaping the antenna's performance. Anisotropy has a more substantial effect on resonances frequency than isotropic substrate. Furthermore, this study is also focused on the effect of the thickness of superconducting antenna patch. It was notable that when the thickness increases, the resonance frequency shows a significant rise. Likewise, we have varied both the thickness of superconducting antenna patch and operating temperature to investigate their effect on the surface resistance and reactance. In the case of varying temperature, the results displayed stability with null values in both surface resistance/reactance at lower temperature (normal state) until it reaches the transition temperature (critical temperature), then it increased swiftly for the other diverse value in the thickness of superconducting antenna patch, while in the case of varying thickness it shows converse to the preceding results associated with the operating temperature. Overall, these exhaustive investigations on the impact of the antenna's key parameters on a superconducting H-shape antenna patch printed on an anisotropic substrate contribute to optimizing the design of our antennas and improving the performance of our structure.

REFERENCES

[1] Boughrara, A. S., S. Benkouda, A. Bouraiou, and T. Fortaki, "Study of stacked high tc superconducting circular disk microstrip antenna in multilayered substrate containing isotropic and/or uniaxial anisotropic materials," *Advanced Electromagnetics*, Vol. 8, No. 3, 1–5, 2019.

[2] Chen, Z. N. and M. Y. W. Chia, *Broadband Planar Antennas: Design and Applications*, John Wiley & Sons, 2006.

[3] Fusco, V. F., *Teoria e Técnicas De Antenas: Princípios e Prática*, 2009.

[4] Balanis, C. A., *Antenna Theory: Analysis and Design*, John Wiley & Sons, 2016.

[5] Sheta, A. F., "A novel H-shaped patch antenna," *Microwave and Optical Technology Letters*, Vol. 29, No. 1, 62–66, 2001.

[6] Gao, S. C., L. W. Li, M. S. Leong, and T. Yeo, "Analysis of an H-shaped patch antenna by using the FDTD method," *Progress In Electromagnetics Research*, Vol. 34, 165–187, 2001.

[7] Palanisamy, V. and R. Garg, "Rectangular ring and H-shaped microstrip antennas — alternatives to rectangular patch antenna," *Electronics Letters*, Vol. 21, No. 19, 874–876, 1985.

[8] Hung, C. C., S. M. Yang, and S. E. Tsai, "On the mechanics of composite structure and electromagnetics of microstrip antenna," *Advances in Mechanical Engineering*, Vol. 10, No. 3, 2018.

[9] Nelson, R. M., D. A. Rogers, and A. G. D'Assuncao, "Resonant frequency of a rectangular microstrip patch on several uniaxial substrates," *IEEE Transactions on Antennas and Propagation*, Vol. 38, No. 7, 973–981, 1990.

[10] Alexopoulos, N. G., "Integrated-circuit structures on anisotropic substrates," *IEEE Transactions on Microwave Theory and Techniques*, Vol. 33, No. 10, 847–881, 1985.

[11] Braaten, B. D., D. A. Rogers, and R. M. Nelson, "Multiconductor spectral domain analysis of the mutual coupling between printed dipoles embedded in stratified uniaxial anisotropic dielectrics," *IEEE Transactions on Antennas and Propagation*, Vol. 60, No. 4, 1886–1898, 2012.

[12] Bedra, R., S. Bedra, and T. Fortaki, "Analysis of elliptical-disk microstrip patch printed on isotropic or anisotropic substrate materials," *International Journal of Microwave and Wireless Technologies*, Vol. 8, No. 2, 251–255, 2016.

[13] Bedra, S., S. Benkouda, R. Bedra, and T. Fortaki, "Characteristics of HTS inverted circular patches on anisotropic substrates," *Journal of Computational Electronics*, Vol. 20, 892–899, 2021.

[14] Bedra, S., R. Bedra, S. Benkouda, and T. Fortaki, "Study of an inverted rectangular patch printed on anisotropic substrates," *IETE Journal of Research*, Vol. 68, No. 2, 1056–1063, 2022.

[15] Bhatnagar, S. K., "New design formulae for equilateral triangular microstrip antenna," *International Research Journal of Engineering and Technology*, Vol. 7, No. 11, 946–952, 2020.

[16] Wang, Z., X. Li, S. Fang, and Y. Liu, "An accurate edge extension formula for calculating resonant frequency of electrically thin and thick rectangular patch antennas with and without air gaps," *IEEE Access*, Vol. 4, 2388–2397, 2016.

[17] Akdagli, A. and A. Toktas, "A novel expression in calculating resonant frequency of H–shaped compact microstrip antennas obtained by using artificial bee colony algorithm," *Journal of Electromagnetic Waves and Applications*, Vol. 24, No. 14-15, 2049–2061, 2010.

[18] Agaba, C., R. Bedra, S. Bedra, S. Benkouda, and T. Fortaki, "Study of superconducting equilateral triangular patch printed on anisotropic dielectric substrates," in *2022 2nd International Conference on Advanced Electrical Engineering (ICAEE)*, 1–6, 2022.

[19] Bedra, S., R. Bedra, S. Benkouda, and T. Fortaki, "Analysis of HTS circular patch antennas including radome effects," *International Journal of Microwave and Wireless Technologies*, Vol. 10, No. 7, 843–850, 2018.

[20] Ustun, D. and F. Toktas, "Surrogate-based computational analysis and design for H-shaped microstrip antenna," *Journal of Electromagnetic Waves and Applications*, Vol. 35, No. 1, 71–82, 2021.

[21] Gao, S. C., L. W. Li, M. S. Leong, and T. Yeo, "Analysis of an H-shaped patch antenna by using the FDTD method," *Progress In Electromagnetics Research*, Vol. 34, 165–187, 2001.

[22] Sheta, A. F., A. Mohra, and S. F. Mahmoud, "Multi-band operation of a compact H-shaped microstrip antenna," *Microwave and Optical Technology Letters*, Vol. 35, No. 5, 363–367, 2002.

[23] Mhamdi, A., S. Bedra, R. Bedra, and S. Benkouda, "CAD cavity model analysis of high Tc superconducting rectangular patch printed on anisotropic substrates," in *2017 5th International Conference on Electrical Engineering — Boumerdes (ICEE-B)*, 1–4, 2017.